Technical Physics Letters, 2023, Vol. 49, No. 9

03.4

# Dynamics of a vapor bubble induced by laser heating of water in a capillary

© A.A. Levin[1,2], D.S. Elistratov[1,3], A.S. Safarov[1,2], A.A. Chernov[1,3]

[1] Novosibirsk State University, Novosibirsk, Russia
[2] Melentiev Energy Systems Institute, Siberian Branch, Russian Academy of Sciences, Irkutsk, Russia
[3] Kutateladze Institute of Thermophysics, Siberian Branch, Russian Academy of Sciences, Novosibirsk, Russia
E-mail: Lirt@mail.ru

Received June 27, 2023
Revised July 14, 2023
Accepted July 15, 2023

The results of an experimental study of the evolution of a laser-induced vapor bubble in a subcooled liquid under spatially constrained conditions (in a capillary) are presented. The influence of geometric parameters on the nature of the process is studied. It was revealed under what conditions the collapse of the bubble is accompanied by the generation of a submerged jet directed from the end of the fiber into the depth of the liquid, and when this does not occur. It is shown that in the latter case, a standing pressure wave is presumably formed in the liquid..

**Keywords:** laser-induced boiling, subcooled liquid, vapor bubble.

DOI: 10.61011/TPL.2023.09.56712.19667

The process of liquid boiling under various conditions has already been examined in a great number of experimental and theoretical papers. Two lines of research are especially relevant at the moment. The first one deals with strongly non-equilibrium and non-stationary boiling processes (including those with changing boundary conditions). The second one is concerned with the phase transition in spatially constrained media where the characteristic size of vapor bubbles is comparable with system dimensions. Both experimental reports, which reveal that known approaches are hardly applicable to the kinetics of nucleation in the conditions of non-stationary heat flows [1], and theoretical papers focused on the development of models of vapor bubble evolution in substantially non-equilibrium conditions [2–4] have already been published. The interest in mini- and microchannel heat-exchange systems is also rising, since they have a wide range of practical applications [5].

The study of laser-induced boiling of a substantially subcooled liquid is another issue of fundamental and applied interest [6–9]. This process is critical for minimally invasive laser surgery, where hot submerged jets produced as a result of collapse of a vapor bubble, which formed in the course of liquid heating by laser radiation, exert thermal and/or mechanical effects on pathogenic tissue and tumors [10]. The process of boiling here is substantially non-stationary with local liquid superheating levels of several hundred degrees. In addition, the liquid volume is naturally limited to values comparable to the volume of emerging vapor inclusions. The evolution of a laser-induced vapor bubble with subsequent generation of a cumulative jet, which becomes submerged further on, has been analyzed both experimentally and theoretically in recent papers [11,12], where this process was examined in a large volume (cuvette). The aim of the present study is to examine laser-induced boiling in a limited volume (capillary) with walls exerting a significant influence on the overall process dynamics.

The experimental setup was described in detail in [12]. The only modification of it is that liquid (distilled water) was introduced in the present study into a glass vertically aligned capillary (capillaries with inner diameters $D_{cap}$ ranging from 3 to 10 mm were used) instead of a cuvette. Water was irradiated with CW laser radiation with a wavelength of $1.94\,\mu$m (the absorption coefficient was $\sim 100\,\text{cm}^{-1}$) transmitted from a laser to the working volume via a quartz-quartz polymer fiber with diameters $d_{fiber} = 0.4$ and 0.6 mm. This provided an opportunity to induce fast local water heating in the vicinity of the end face of the fiber, which led to explosive nucleation of a vapor embryo. This embryo evolved through the stages of rapid growth and subsequent (no less rapid) collapse accompanied by the formation of a submerged liquid jet. The radiation power was varied from 2 to 10 W in 1 W increments. The water temperature was kept constant at $30 \pm 2°$C. The pressure in the system was atmospheric. A high-speed Photron FASTCAM Mini UX100 camera with a frame rate up to 100 000 fps was used to record the examined process. The error of measurement of bubble sizes did not exceed $32\,\mu$m.

Figure 1 presents the frame-by-frame evolution of vapor structures forming upon absorption of laser radiation by water at different ratios between capillary diameter $D_{cap}$ to fiber diameter $d_{fiber}$. Successive stages of nucleation (Fig. 1, $b$, frames 2, 3), growth (Fig. 1, $b$, frames $3-15$), and collapse (Fig. 1, $b$, frames $15-29$) of a vapor bubble are seen clearly. Note that the growth of a bubble is maintained by evaporation of liquid that was superheated locally by laser radiation (at the induction stage). According to the results of calculations [12], the temperature of liquid at the

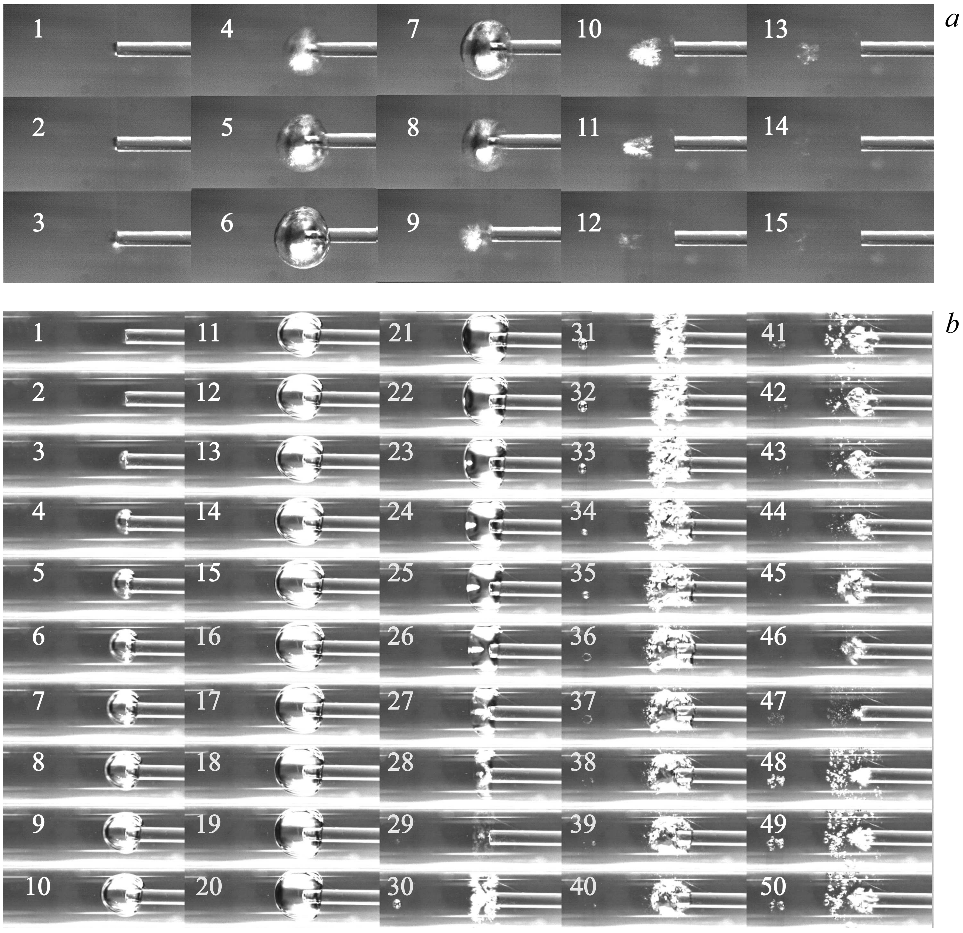


**Figure 1.** Dynamics of vapor structures forming upon absorption of laser radiation by water in capillaries of various diameters. $a$ — $D_{cap} = 10\,\mathrm{mm}$, $d_{fiber} = 0.4\,\mathrm{mm}$; $b$ — $D_{cap} = 3\,\mathrm{mm}$, $d_{fiber} = 0.6\,\mathrm{mm}$. The laser radiation power is 10 W. The time interval between frames is $40\,\mu$s.

moment of bubble nucleation (localized to the nucleation spot) exceeds considerably the saturation temperature and is close to the superheat-limit temperature. The collapse of a bubble is induced by the overall liquid subcooling and is accompanied by vapor condensation. If the capillary diameter exceeds considerably the fiber diameter (Fig. 1, $a$), the scenario of bubble growth is almost the same as the one seen when a laser-induced bubble evolves in a large liquid volume [11,12]. This process is specific in that the shape of a bubble remains near-spherical throughout its growth and collapse (with the possible exception of the last moments of its existence). The collapse of a bubble is then accompanied by the generation of a hot submerged jet directed from the fiber end into the depth of the liquid [11,13].

In the present study, we examine another scenario with the difference between the capillary diameter and the fiber diameter being less significant. The bubble growth transverse to the capillary axis is limited in this scenario by the capillary walls, and the spherical shape of a bubble is not retained in the process of growth. Reaching its maximum size, a bubble blocks completely the cross section of the capillary. The hydrodynamic pattern is then altered substantially relative to the one found in the scenario of bubble growth in a large volume. Specifically, with the transverse motion of liquid being infeasible, the bubble collapse proceeds under a significant velocity asymmetry of liquid flowing to the boundary surface. It is evident that the liquid velocity reaches its maximum at the capillary axis. This is seen clearly in frames 22–27 (Fig. 1, $b$): a characteristic deep cavity facing the fiber end forms in the bubble. It is appropriate here to draw an analogy with the bubble collapse near a plane surface (see, e.g., [7]), where a similar scenario is actualized. Note that, in contrast to experiments on boiling in a large volume, a submerged jet directed from the fiber end into the depth of the liquid does not form in this case, since the required conditions are not established.

It can be seen from Fig. 1, $b$ that the bubble collapse induces pressure pulsations in the liquid, which initiate a cyclic process of formation and condensation of the vapor phase (frames 29–47) with a period of $\sim 0.72\,\mathrm{ms}$. Oscillations of a „parasitic“ gas bubble located at a distance of 6 mm from the fiber end provide an additional illustration of this. It should be noted that pressure pulsations are also

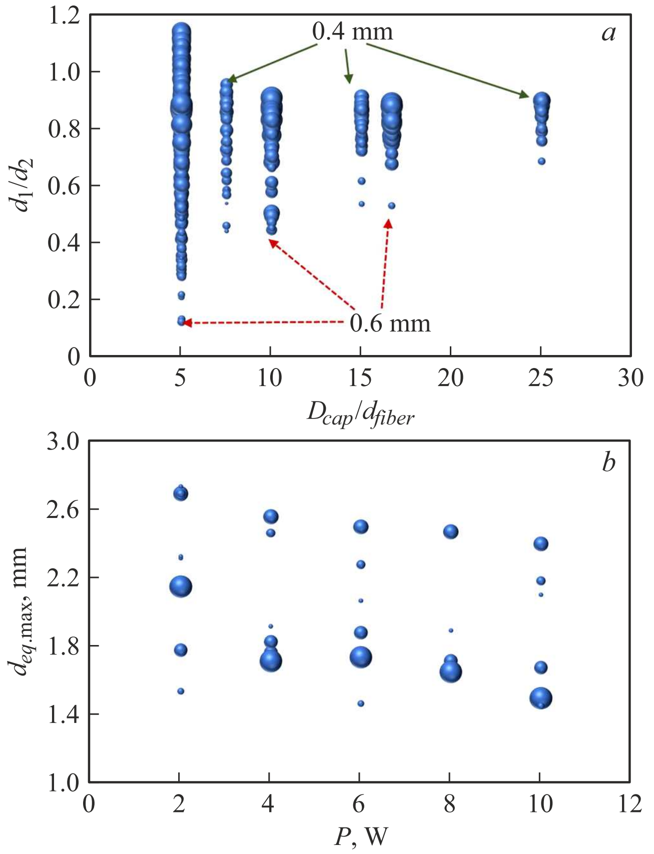


**Figure 2.** Geometric parameters of a vapor bubble in the process of its evolution. *a* — Bubble ellipticity for different ratios of diameters of the fiber and the capillary; the marker size is proportional to the equivalent bubble diameter (i.e., the diameter of a sphere with its volume equal to the one measured for a vapor bubble in video frames). *b* — Dependence of the maximum vapor bubble size ($d_{eq.\max}$) on laser radiation power $P$; the marker size is proportional to geometric factor $\delta$.

observed in large-diameter capillaries and a large volume, but their amplitude there is significantly lower than the one in small-diameter capillaries. It is fair to assume that, when a bubble collapses in a large volume, a considerable fraction of the kinetic energy of liquid is spent on the formation of a submerged jet instead of a standing pressure wave.

Thus, the scenarios of evolution of laser-induced bubbles in capillaries of different diameters differ radically and are shaped by the influence of capillary walls on the liquid flow pattern around a bubble. This influence is manifested primarily in the loss of sphericity of a bubble (especially evident when the bubble size becomes comparable to the capillary diameter) in the course of its growth and leads to different scenarios of evolution of the vapor–liquid system.

A dependence of ellipticity coefficient (naturally, this term is not used in its strict mathematical sense) $k = d_1/d_2$, which is the ratio of longitudinal bubble dimension $d_1$ to transverse dimension $d_2$, on the degree of confinement of a bubble in the capillary, which was characterized by the geometric factor (ratio of capillary diameter $D_{cap}$ to fiber diameter $d_{fiber}$: $\delta = D_{cap}/d_{fiber}$), was plotted to summarize the results obtained in a series of experiments (Fig. 2, *a*). It can be seen that the range of $k$ values is extended considerably at smaller $\delta$. This implies that the bubble shape ceases to be spherical. Specifically, ellipticity $k = 1.2$ (Fig. 1, *b*, frame 21) in capillaries with a relatively small diameter ($\delta = 5$) when a bubble reaches its maximum size and effectively turns into a „projectile on a fiber." At the moment when its collapse is almost over, $k = 0.12$ (Fig. 1, *b*, frame 28). A different pattern is observed in large-diameter capillaries ($\delta = 25$), where a bubble grows in almost unconstrained conditions and the range of $k$ variation is less significant.

Let us examine the influence of the radiation power on the maximum size of a growing bubble, since the latter parameter largely predetermines the subsequent development of the process. This size was characterized by the maximum equivalent diameter, which is the diameter of a sphere with its volume equal to the one measured for a vapor bubble in video frames. As was demonstrated in [12] via numerical modeling, the bubble size decreases somewhat if the radiation power increases significantly; at the same time, this size depends to a considerable extent on the diameter of a fiber at the end of which a locally superheated liquid boils. Comparing the bubbles (Fig. 2, *a*) produced at the end of fibers with various diameters, one may note that the maximum sizes of bubbles at $d_{fiber} = 0.6$ mm are significantly greater than those at $d_{fiber} = 0.4$ mm. This verifies the hypothesis proposed earlier and is ultimately attributable the difference in thermal energy reserves accumulated by the liquid at the induction stage.

Figure 2, *b* illustrates the experimental dependence of the maximum bubble size on the laser radiation power at different values of $\delta$. It can be seen that the dependence at large $\delta$ is similar to the one observed for bubbles growing in a large volume [12]: the size is inversely proportional to radiation power. However, this monotonicity vanishes as geometric factor $\delta$ decreases (i.e., the free space available for growth of a vapor bubble shrinks). Apparently, this is indicative of a reduced stability of boiling in constrained conditions, since even a slight change in the spatial localization of a vapor embryo has a significant effect on the hydrodynamic pattern and, consequently, the maximum vapor bubble size.

Summarizing the foregoing, one may state that the process conditions need to be known exactly if the process of laser-induced liquid boiling is to be used in practice, since different scenarios of boiling may be realized depending on these conditions. Specifically, if one intends to utilize the effect of generation of submerged liquid jets upon collapse of vapor bubbles, it appears reasonable to avoid low values of geometric factor $\delta$, since these jets may not form at all in constrained conditions. As for the laser radiation power, it does not exert any significant influence on the processes of boiling and generation and propagation of submerged liquid jets in a large volume, but provides an opportunity to adjust the maximum size of a growing vapor bubble (within a range relevant to practical applications) in constrained conditions.

### Funding

This study was supported by the Russian Science Foundation (project No. 22-19-00092).

### Conflict of interest

The authors declare that they have no conflict of interest.

## References

[1] A.A. Levin, P.V. Khan, Appl. Therm. Eng., **149**, 1215 (2018). DOI: 10.1016/j.applthermaleng.2018.12.126
[2] A.A. Avdeev, *Bubble systems* (Springer, Cham, 2016).
[3] A.A. Chernov, A.A. Pil'nik, I.V. Vladyko, S.I. Lezhnin, Sci. Rep., **10** (1), 16526 (2020). DOI: 10.1038/s41598-020-73596-x
[4] L. Zhang, H. Liu, D. Chen, X. Zhou, Y. Chen, Int. J. Heat Mass Transfer, **176**, 121426 (2021). DOI: 10.1016/j.ijheatmasstransfer.2021.121426
[5] D. Deng, L. Zeng, W. Sun, Int. J. Heat Mass Transfer, **175**, 121332 (2021). DOI: 10.1016/j.ijheatmasstransfer.2021.121332
[6] J.P. Padilla-Martinez, C. Berrospe-Rodriguez, G. Aguilar, J.C. Ramirez-San-Juan, R. Ramos-Garcia, Phys. Fluids, **26** (12), 122007 (2014). DOI: 10.1063/1.4904718
[7] M. Mohammadzadeh, S.R. Gonzalez-Avila, K. Liu, Q.J. Wang, C.-D. Ohl, J. Fluid Mech., **823**, R3 (2017). DOI: 10.1017/jfm.2017.358
[8] S.D. George, S. Chidangil, D. Mathur, Langmuir, **35** (31), 10139 (2019). DOI: 10.1021/acs.langmuir.8b03293
[9] A. Brujan, H. Takahira, T. Ogasawara, Exp. Therm. Fluid Sci., **101**, 48 (2019). DOI: 10.1016/j.expthermflusci.2018.10.007
[10] V.P. Minaev, N.V. Minaev, V.Y. Bogachev, K.A. Kaperiz, V.I. Yusupov, Lasers Med. Sci., **36** (8), 1599 (2021). DOI: 10.1007/s10103-020-03184-y
[11] V.M. Chudnovskii, A.A. Levin, V.I. Yusupov, M.A. Guzev, A.A. Chernov, Int. J. Heat Mass Transfer, **150**, 119286 (2020). DOI: 10.1016/j.ijheatmasstransfer.2019.119286
[12] A.A. Chernov, A.A. Pil'nik, A.A. Levin, A.S. Safarov, T.P. Adamova, D.S. Elistratov, Int. J. Heat Mass Transfer, **184**, 122298 (2022). DOI: 10.1016/j.ijheatmasstransfer.2021.122298
[13] V.I. Yusupov, Tech. Phys. Lett., **48** (10), 9 (2022). DOI: 10.21883/TPL.2022.10.54788.19301.

*Translated by Ego Translating*